Pertanika J. Sci. & Technol. 33 (2): 639 - 651 (2025)

PERTANIKA JOURNALS

SCIENCE & TECHNOLOGY

Journal homepage: http://www.pertanika.upm.edu.my/

Simulation of Solar Charge Controller Module with Current Backflow Protection

Aimi Dalila Azhar[1]*, Weng Ho Yew[2], Akmal Zaini Arsad[2], Azrul Ghazali[1], Fazrena Azlee Hamid[1] and Ahmad Wafi Mahmood Zuhdi[1,2]

[1]College of Engineering, Universiti Tenaga Nasional (UNITEN), Kajang 43000, Selangor, Malaysia
[2]Institute of Sustainable Energy, Universiti Tenaga Nasional (UNITEN), Kajang 43000, Selangor, Malaysia

ABSTRACT

Solar energy is popular worldwide due to the escalating demand for renewable and clean energy solutions. The inherent low power conversion efficiency of solar panels highlights the indispensable role of a solar charge controller in optimizing the power transfers from the solar panel to a storage battery. Traditional buck converters are marred by considerable power losses due to freewheeling diodes, thus making a synchronous buck converter, which necessitates protection against the reverse current from the battery to the solar panel. During low irradiation, the solar panel voltage typically falls below the battery voltage, creating the potential for reverse current flow, which may cause damage to other system components. This study proposes an innovative current backflow protection circuit, effectively addressing reverse polarity risks, demonstrated through LTspice simulations. Utilizing an NMOS MOSFET, this circuit disrupts the connection whenever solar panel voltage falls beneath a predefined cutoff value, thereby preventing reverse current damage. The protective mechanism's efficacy is validated by monitoring the NMOS MOSFET's drain current, which remains at 0A below the cutoff voltage but transitions to negative values above it, indicating a reverse flow and underscoring the circuit's reliability in safeguarding solar energy systems.

Keywords: Current backflow, cutoff MOSFET, protection circuit, solar charge controller, undervoltage

ARTICLE INFO

Article history:
Received: 4 April 2024
Accepted: 1 October 2024
Published: 21 February 2025

DOI: https://doi.org/10.47836/pjst.33.2.05

E-mail addresses:
aimi.dalila@uniten.edu.my (Aimi Dalila Azhar)
whyew97@hotmail.com (Weng Ho Yew)
akmalzaini@uniten.edu.my (Akmal Zaini Arsad)
azrulg@uniten.edu.my (Azrul Ghazali)
Fazrena@uniten.edu.my (Fazrena Azlee Hamid)
Wafi@uniten.edu.my (Ahmad Wafi Mahmood Zuhdi)
*Corresponding author

INTRODUCTION

Solar energy is one of the abundant resources that can be harvested to meet energy demands following the sustainable energy solution. Solar photovoltaic (PV) systems have become an important component of renewable energy, generating electricity for

ISSN: 0128-7680
e-ISSN: 2231-8526

a wide array of applications, from residential rooftops to large-utility installations (Breyer et al., 2021). A solar charge controller (SCC) is responsible for ensuring that solar energy is optimally converted into electricity, increasing the efficiency of the system (Rokonuzzaman et al., 2020). Typically, a SCC uses buck converter topology to step down the voltage from the solar panel to the battery. Figure 1(a) presents a conventional buck converter consisting of a MOSFET, a freewheeling diode, an inductor, and a capacitor. The freewheeling diode has caused a significant loss from the voltage drop across it (Zomorodi & Nazari, 2022). A synchronous buck converter was used to replace the diode with an active component, such as a MOSFET, as shown in Figure 1(b), to address this issue.

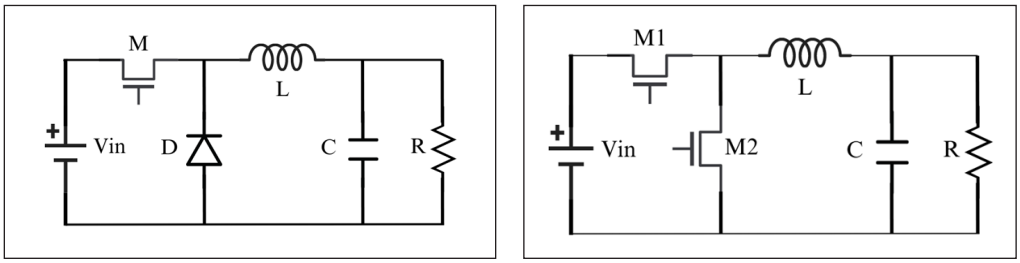

(a) (b)

Figure 1. Circuit diagram of (a) conventional buck converter and (b) synchronous buck converter

The synchronous buck converter, however, has a few drawbacks. Switching losses occur during the switching of the MOSFETs depending on the frequency of the converter (Eraydin & Bakan, 2020). Lee et al. (2015) improved up to 7% efficiency by introducing a zero-voltage resonant-transition switching on a GaN-based synchronous buck converter. The resonant transition ensures the MOSFET is turned on and off when only the voltage across it is zero or nearly zero. Kumar et al. (2015) used a simple passive auxiliary circuit to reduce the stress caused by the switching action and can improve the efficiency of the synchronous buck converter. Therefore, proper gate driver circuitry and MOSFET selection are crucial to minimizing the switching losses.

On the other hand, a synchronous buck converter also requires circuit protection since the presence of passive components like an inductor and capacitor may create a potential for voltage spike and current surge (Muntaser et al., 2022). Wang et al. (2016) proposed a fast overcurrent detection method that limits the inductor peak current during short circuit cases. This applied method is able to protect the devices from any damage caused by the overcurrent. Guo et al. (2019) used a current-constraint controller to work with a disturbance observer to limit the inductor current whenever a disturbance occurred. A peak current detection with an in-built maximum current limiter was offered by Deo et al. (2022) again to limit the inductor's current. Hammerbauer and Stork (2021) acknowledged that an

overvoltage might happen during sudden load disconnects. They used a comparator after the inductor or simply a Zener diode to protect the transistor of the buck converter for a low-power converter application. Nevertheless, these overvoltage solutions only address the problems related to the load.

The inductor in the buck converter keeps charging and discharging while storing energy in the form of a magnetic field during the switching process. When energy is released during discharging, a reverse current may occur, which flows in the opposite direction (Marouchos, 2006). Besides, a reverse current might also happen during a lack of irradiation, in which the voltage extracted from the solar panel is lower than the voltage supplied to the battery. This phenomenon typically occurs in dual-active-bridge (DAB) converters, which reduces the converter's efficiency (Xu et al., 2022). Since the DAB converter is a dual-flow converter, the power backflow needs to be minimized instead of prevented. The reverse current that flows from the battery to the solar panel may cause damage to the components of the buck converter. Raghavendra and Padmavathi (2018) acknowledged that the reverse polarity of the battery may have caused this phenomenon. Hence, they used a transistor to detect the polarity of the battery and turn a MOSFET OFF when it is reversed. Kumar et al. (2018) utilized a MOSFET to block the current from the battery whenever the battery is fully charged, as indicated by an LED. Meanwhile, Gupta et al. (2022) implemented a relay to disconnect the battery from the system.

To the best of our knowledge, no work has been conducted to overcome the problem of current backflow from the load to the solar panel specifically caused by under-voltage at the input side. Most of the literature discussed monitoring the status of the battery before disconnecting it, while current backflow might happen before the battery is fully charged, which is during low irradiation. Therefore, this paper addresses the issue of current backflow that typically occurs in synchronous buck converters due to a drop in the input voltage compared to the output. A 50W solar panel with a maximum voltage of 20V and a 12V lead acid battery is used. A predefined offset value of 15V is set as the minimum voltage of the solar panel before the protection circuit disconnects the solar panel from the whole system. MPPT algorithm is not the main focus of this study since the issue is on the current backflow.

MATERIALS AND METHODS

Buck Converter

From this discussion onwards, the input voltage term is used to mention voltage from the solar panel, while output voltage for voltage is supplied to the battery. A circuit diagram of a conventional buck converter is portrayed in Figure 1(a). It consists of a MOSFET (M), a freewheeling diode (D), an inductor (L), a capacitor (C), and a load (R). When MOSFET M1 is ON, the current will flow from the input voltage to the load through the

inductor. When it is OFF, the current will flow through the diode, and since a diode has a high voltage drop of around 0.7V, it will cause a conduction loss that will lead to efficiency reduction. A lower-side MOSFET, M2, is used to replace the diode in a synchronous buck converter, as displayed in Figure 1(b), which will reduce the drop typically around 0.3V or less, therefore increasing the power efficiency by 5% or higher (Eraydin & Bakan, 2020).

Current Backflow in Synchronous Buck Converter

During dawn, dusk, and night times, where low irradiance times and places, the voltage from the solar panel has the potential to be lower than the battery voltage, thus causing a current backflow from the battery to the panel. In a synchronous buck converter, a large reverse current flow might happen when the output voltage is higher than the input voltage, and the output capacitance is modeled as the battery is large (Wang et al., 2019). The reverse current from the inductor, $I_{L,\ reversed}$ during discharging, and the reverse current that flows through the body diode of M1, $I_{M1,\ reversed}$ during the OFF state, produced around three to four times the amount that flows through the inductor, as portrayed in Figure 2, therefore damaging the M2. Compared to a conventional buck converter, the current backflow is most unlikely to happen because of the presence of the freewheeling diode that blocks any current flow from the opposite direction.

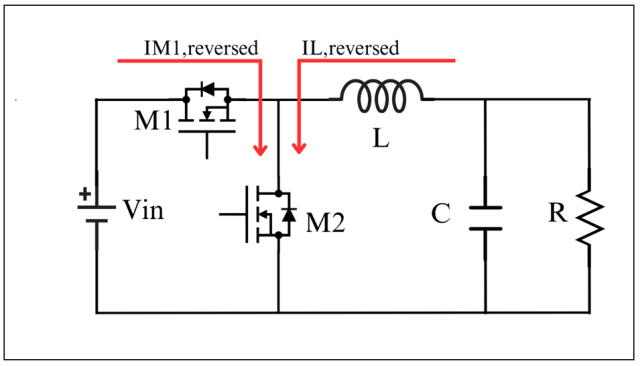

Figure 2. Reverse current is caused by reverse current from the inductor and transistor (M1) body diode

Current Backflow Protection Circuit

In this paper, a protection circuit is designed to address the issue of the current backflow in a synchronous buck converter. The circuit is placed between the input voltage and the buck converter, as shown in Figure 3. The buck converter circuit will be disconnected from the solar panel when the solar panel voltage falls below a predefined offset value. The offset value of 15V was chosen, as it is slightly higher than the maximum charging voltage of the battery, which is 14.8V. Simulation using LTspice was conducted to analyze

the behavior of the circuits under various conditions, with components modeled based on real components to ensure circuit functionality.

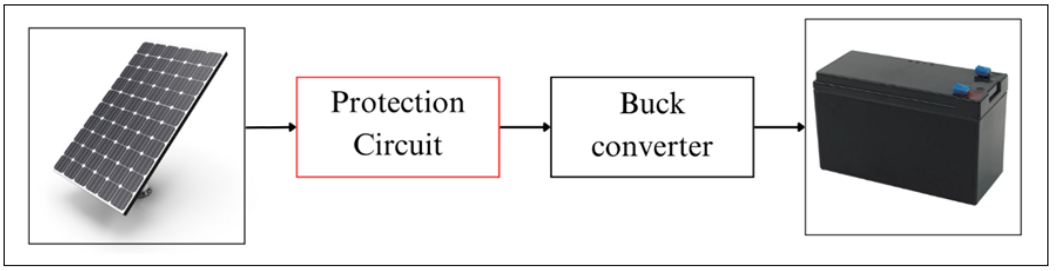

Figure 3. Block diagram of the proposed system

Figure 4 shows the circuit diagram of the protection circuit. Vpanel represents the input voltage from the solar panel, while Vbuck represents the voltage of the synchronous buck converter circuit. M3, on the other hand, is the cutoff NMOS MOSFET that will connect and disconnect the converter circuit. Vcc is set to 12V, while Vpc is voltage-dependent on the Vpanel value. Besides, the gate voltage of M4, Vg_{M4} and M4 depends on Vpc. In other words, the state of M4 depends on the value of Vpanel.

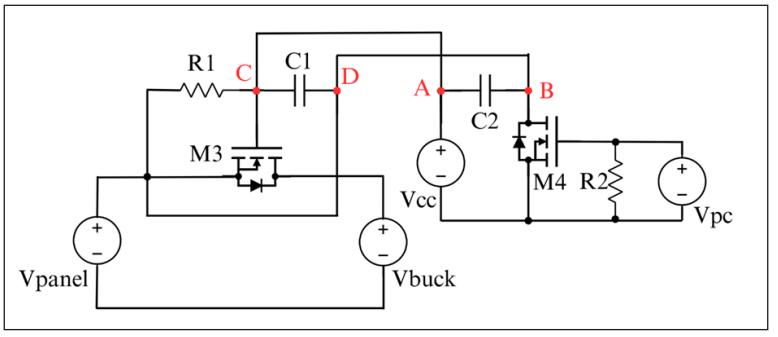

Figure 4. Current backflow protection circuit

For the first case where Vpanel ≥ 15V, M4 will be ON and shorted to ground, thus introducing a voltage difference between Node A and B. Since Node C is equal to Node A, while Node D is equal to Node B, they will have the same value. The voltage difference is good enough to make M3 ON and thus connect the solar panel from the buck converter. On the other hand, for the second case where Vpanel < 15V, Vpc is inadequate to supply enough voltage to Vg_{M4}. M4 is OFF and causes the same voltage at Node A and B. The same voltage value is insufficient to make M3 ON, thus disconnecting the solar panel from the buck converter.

RESULTS AND DISCUSSION

Synchronous Buck Converter

A synchronous buck converter consists of two MOSFETs, an inductor, and a capacitor at the output, as shown in Figure 5. An NMOS (IRFZ44N, Infineon) with a threshold voltage, V_{th} of 4V, was selected because it has low on-state resistance and fast switching speed that are suitable for use by a switching converter. The gate signals are given a PWM signal with a 50% duty cycle driven by a gate driver that uses a push-pull configuration. The gate driver contains a bootstrap capacitor, C2, that will introduce a delay to produce a dead time to minimize the switching losses.

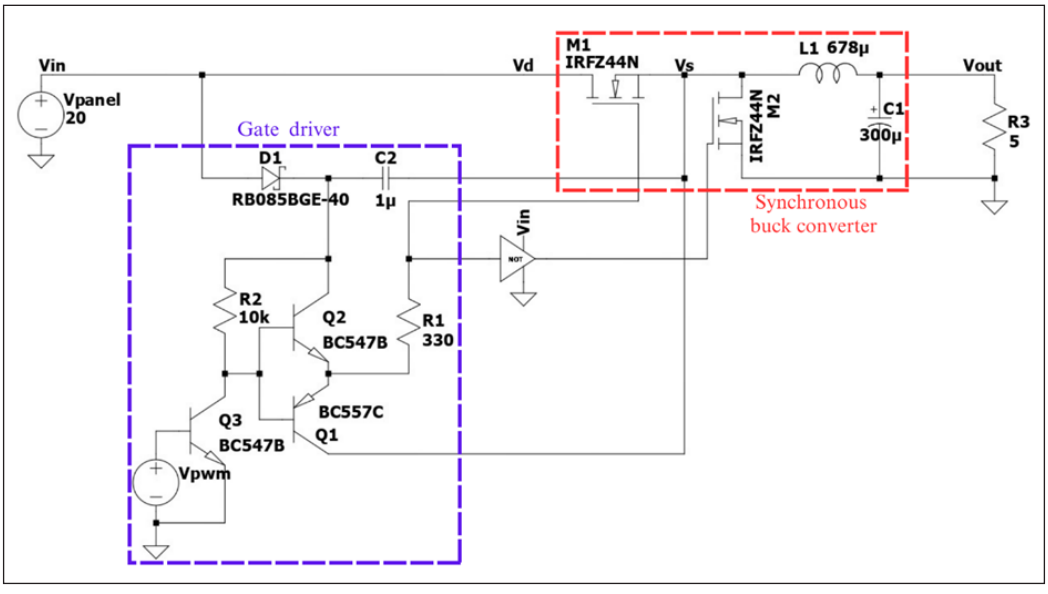

Figure 5. Synchronous buck converter circuit in LTspice

Figure 6(a) shows the voltage transfer function of the synchronous buck converter by sweeping the Vpanel from 0V to 20V. The linear graph starts at 4V panel voltage, which indicates the need to exceed the V_{th} of the M1 to operate the converter. The same model is simulated again for a transient time of 30ms, and the Vpanel is set to constant 20V. The output response (Vout) is shown in Figure 6(b). The graph shows that the circuit took around 9ms for the output voltage to achieve a steady state voltage of 9.43V. The slightly lower voltage from the estimated 50% duty cycle is due to conduction losses from the NMOS (Eraydin & Bakan, 2020). It shows that the synchronous buck converter has a small power drop with a power efficiency of 94.3%.

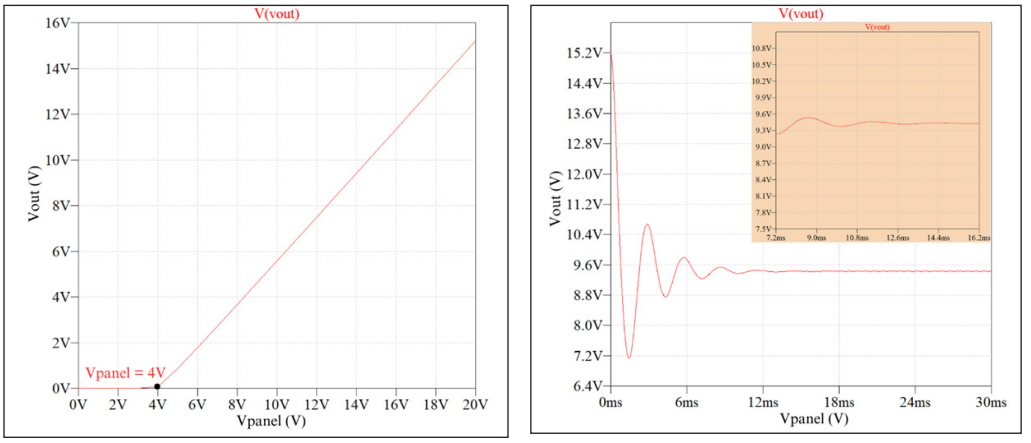

(a) (b)

Figure 6. Output voltage of synchronous buck converter for (a) panel voltage from 0V to 20V, and (b) panel voltage at 20V in 30ms

Current Backflow Protection Circuit

The proposed protection circuit in Figure 4 was previously implemented in LTspice, as shown in Figure 7. M3 uses NMOS (CSD17506, Texas Instrument) with $V_{TH,}$ M3 of 1.6V as the cutoff NMOS because it has the lowest drift in $R_{DS,}$ on over operating temperature range. M4 uses NMOS (Si2316DS, Vishay) with a threshold voltage, $V_{TH,M4}$ of 2.1V. When Vpanel < 15V, the V2 will supply Vg, M4 is lower than $V_{TH,M4}$, and thus, M4 is turned OFF. An additional resistor, R2, is added in series with a voltage source to make it a current source from the solar panel for better analysis in LTspice.

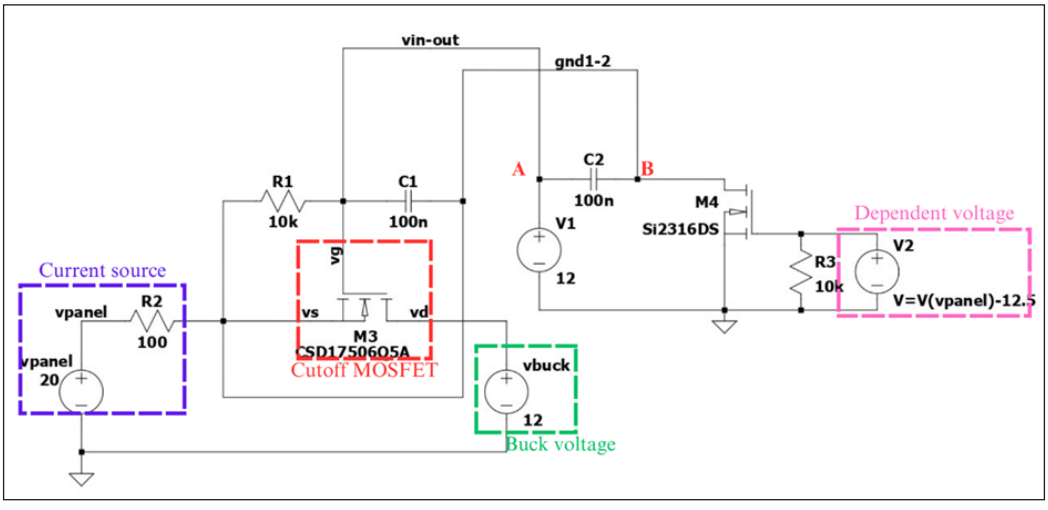

Figure 7. LTspice model of backflow current protection circuit

Figure 8(a) below shows the gate-to-source V_{GS} of M3 for panel voltage from 0V to 20V. At 15V Vpanel, M3 is turned ON after V_{GS} reaches the $V_{TH,M3}$, which is 1.7V. The drain current I_D, meanwhile, is shown in Figure 8(b) for the same panel voltage. In the OFF region where the Vpanel <15V, no current flows out of the M3. At 15V Vpanel, the M3 starts to ON, and the current starts to flow. This proves that the M3 is able to block the reverse current flowing from the buck converter to the solar panel in the OFF region.

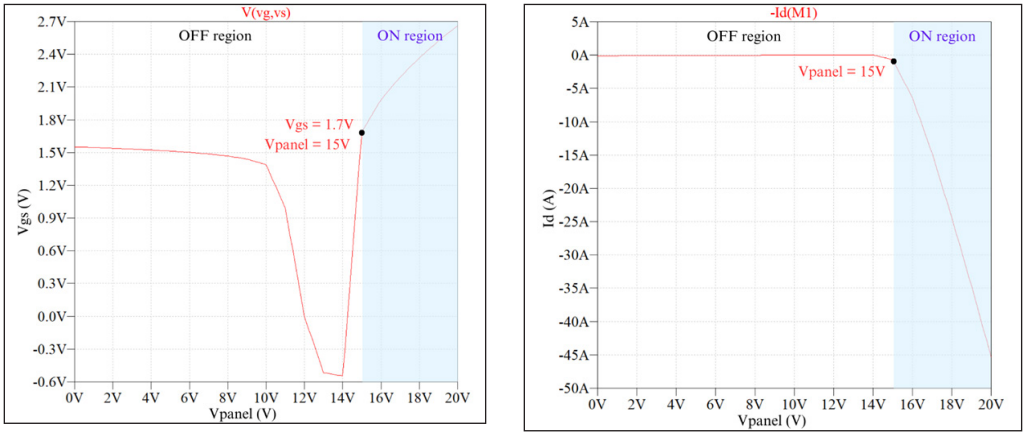

(a) (b)

Figure 8. (a) VGS and (b) ID of M3 for backflow current protection circuit

Synchronous Buck Converter with Current Backflow Protection Circuit

Figure 9 shows the integration of the synchronous buck converter and backflow current protection circuit in LTspice. The protection circuit is located between the voltage source and the synchronous buck converter. Initially, the model is simulated without a battery model first. Figure 10(a) shows the I_D of M3 to monitor the ON/OFF state of the NMOS. M3 has a leakage current of 1μA; therefore, M3 is assumed to be ON when I_D is more than 1μA. From Figure 10(a), the M3 is ON when Vpanel<15V while OFF when Vpanel>15V, which is supposedly ON only when the Vpanel is more than 15V.

Therefore, a battery model is inserted as the load of the buck converter to force an almost constant 12 voltage. The I_D current is presented in Figure 10(b), showing the current is almost 0A for Vpanel<15V, indicating the OFF state of M3. Then, it decreases to almost -6A after the Vpanel reaches 15V, indicating the ON state of M3. The ON and OFF regions with the additional battery model are now swapped (Figure 10). It shows that reverse current might not happen when there is no battery as the load. This battery introduced a voltage difference that led to a reverse current, as shown in Figure 10(b).

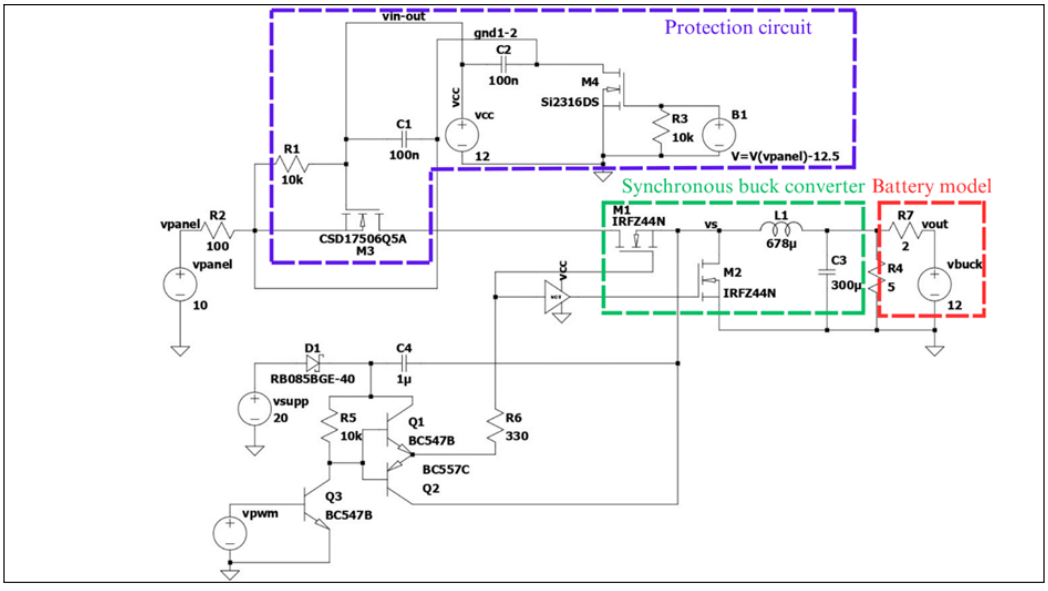

Figure 9. Synchronous buck converter with protection circuit in LTspice

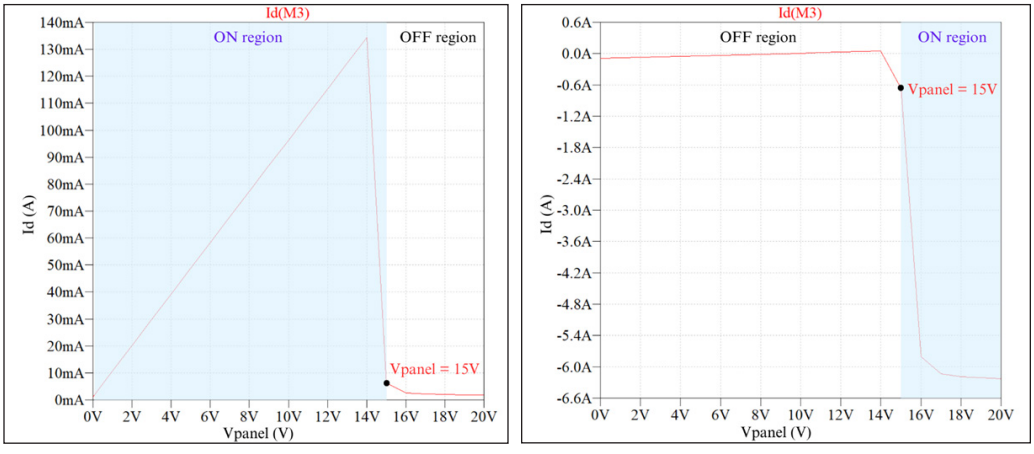

(a) (b)

Figure 10. Drain current of M3 for a synchronous buck converter with protection circuit (a) without battery model, and (b) with battery model

Validation of the Results

Model validation was performed by inserting the current backflow protection circuit into a solar charge controller module prototype. The prototype was then tested under a controlled condition to replicate a low irradiance condition. Further testing under real operating conditions will be conducted and reported in a separate manuscript. Figure 11 shows the

response of the input current when the input voltage is beneath the predefined offset voltage during a period of low irradiation (300W/m^2). The input current fell to 0A when the input voltage started to drop towards 15V. The current was maintained at 0A until the voltage rose steadily beyond 15V.

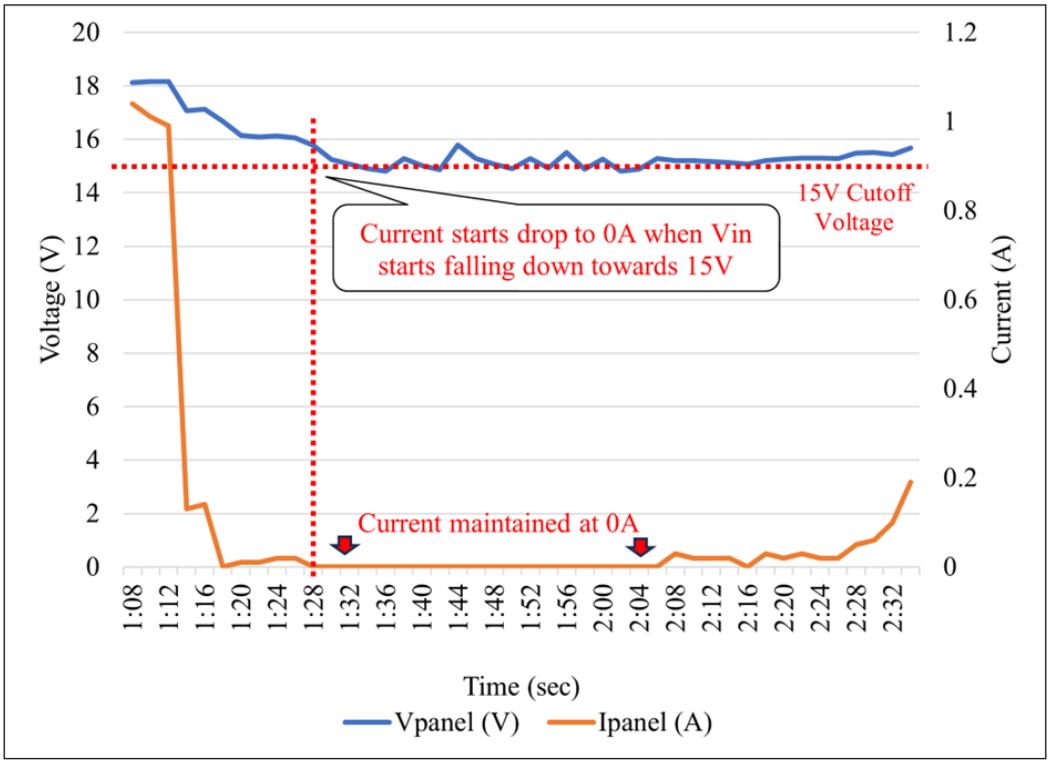

Figure 11. Input current response to the input voltage

Discussion of the Results

A synchronous buck converter was successfully simulated in LTspice. The output voltage gives a value once the input voltage exceeds the MOSFET's V_{TH}. The buck converter steps down the input voltage with an efficiency of 94.3%. A current source is used as the input to monitor the system's current flow. The current starts giving a value after the input voltage exceeds the predefined offset value of 15V. The current is in negative values, showing that the current is flowing in the opposite direction.

After passing the functionality test of the individual circuit, the protection circuit is integrated into the synchronous buck converter. At first, the converter seems to be ON for 0V < input voltage < 15V. The voltage at Vd of M3 is no longer a 12V, as constructed in Figure 7, because it depends on the input voltage values. Consequently, a 12V battery model is inserted as the circuit's load to force a constant 12V at Vd. The converter is simulated

again and shows different behavior. The output current starts giving negative values after the input voltage achieves 15V. The proposed protection circuit can block the reverse current when the input voltage is below the predefined offset value of 15V.

Compared to the output voltage of the synchronous buck converter without circuit protection in Figure 6, the buck converter is operated when the panel voltage reaches the threshold voltage, which is 4V. Meanwhile, a protection circuit is introduced only to let the buck converter operate after the panel voltage reaches the predefined offset voltage of 15V, as shown in Figure 10. From Figure 10, the current is flowing in the reverse direction. Therefore, for Vpanel<15V, the protection circuit can block the reverse current by disconnecting the solar panel from the synchronous buck converter. In addition, the model was validated by using a prototype. The protection circuit was proven to disconnect the solar panel from the buck converter whenever the input voltage drops below 15V.

CONCLUSION

This paper introduces a protection circuit with a synchronous buck converter strategically designed to mitigate the challenges associated with current backflow during low irradiance and nighttime operation. The proposed circuit works by turning off the cutoff NMOS MOSFET M3 and consequently shutting down the converter when the panel voltage falls below the predefined offset voltage of 15V. This protective mechanism is achieved through the introduction of a specific potential difference at the gate and source of M3. The proposed protection circuit has been simulated using the LTspice software. Using the available market components in the simulation, the proposed model shows a promising result in preventing current backflow in synchronous buck converter. The design was also validated through a prototype, which proved the proof-of-concept of the protection circuit.

Using a highly efficient topology, a synchronous buck converter, brings many benefits to a solar charge controller application. However, timing plays a critical role in determining the operation of the converter. During the simulation, the timing of the upper-side and lower-side MOSFET (M1 and M2) can work synchronously, but not in the implementation. It comes with the role of the gate driver to ensure the MOSFETs switch quickly and efficiently. Other than that, having four MOSFETs in a controller will increase heat dissipation. Ineffective thermal management will cause higher temperatures and lead to higher losses, further damaging the components. Lastly, changing the type of MOSFETs (M3 and M4) might produce different results because the protection circuit depends on the V_{TH} value of the MOSFET. Different MOSFET has different V_{TH} values.

The next phase of the research involves establishing a hardware model to experimentally verify the robustness and real-world applicability of the proposed protection circuit. This validation process by using the hardware model is crucial for confirming the reliability and performance of the circuit in practical scenarios, considering factors such as

component tolerances, temperature variations, and transient conditions. Future work also could explore enhancing the circuit's efficiency, reducing power losses, or adapting it for specific application scenarios. Additionally, comprehensive testing under diverse operating conditions will contribute to a more thorough understanding of the circuit's behavior.

ACKNOWLEDGEMENT

The authors acknowledged the support of the Institute of Sustainable Energy (ISE) of Universiti Tenaga Nasional and UNITEN R&D Sdn. Bhd. for continuous support through the TNB Seeding fund U-TE-RD-18-01.

REFERENCES

Breyer, C., Bogdanov, D., Khalili, S., & Keiner, D. (2021). Solar photovoltaics in 100% renewable energy systems. In Meyers, R. A. (Ed.), *Encyclopedia of Sustainability Science and Technology* (pp. 1-30). Springer. https://doi.org/10.1007/978-1-4939-2493-6_1071-1

Deo, A., Maity, A., & Patra, A. (2022). A voltage-emulated peak current controlled buck converter for automotive applications with in-built over-current protection. *Microelectronics Journal*, *123*, Article 105423. https://doi.org/10.1016/J.MEJO.2022.105423

Eraydin, H., & Bakan, A. F. (2020). Efficiency comparison of asynchronous and synchronous buck converter. In *2020 6th International Conference on Electric Power and Energy Conversion Systems (EPECS)* (pp. 30-33). IEEE Publishing. https://doi.org/10.1109/ICPERE.2012.6287236

Guo, T., Huang, S., & Wang, X. (2019). Overcurrent protection control design for DC-DC buck converter with disturbances. *IEEE Access*, *7*, 90825–90833. https://doi.org/10.1109/ACCESS.2019.2926985

Gupta, P. P., Kumar, N., & Nangia, U. (2022). Passive cell balancing and battery charge controller with CCCV topology. In *2022 3rd International Conference for Emerging Technology (INCET)* (pp. 1-5). IEEE Publishing. https://doi.org/10.1109/INCET54531.2022.9825104

Hammerbauer, J., & Stork, M. (2021). Output overvoltage in DC-DC switching converters in case of sudden unloading. In *2021 International Conference on Applied Electronics (AE)* (pp. 1-4). IEEE Publishing. https://doi.org/10.23919/AE51540.2021.9542875

Kumar, P., Sinha, P., Roy, C., & Basu, M. (2018). Design and implementation of solar charge controller for photovoltaic systems. *ADBU-Journal of Engineering Technology*, *7*(1), 1-4.

Kumar, S. S., Panda, A. K., & Ramesh, T. (2015). A ZVT–ZCT PWM synchronous buck converter with a simple passive auxiliary circuit for reduction of losses and efficiency enhancement. *Ain Shams Engineering Journal*, *6*(2), 491–500. https://doi.org/10.1016/J.ASEJ.2014.10.018

Lee, W., Han, D., Morris, C., & Sarlioglu, B. (2015). Minimizing switching losses in high switching frequency GaN-based synchronous buck converter with zero-voltage resonant-transition switching. In *2015 9th International Conference on Power Electronics and ECCE Asia (ICPE-ECCE Asia)* (pp. 233-239). IEEE Publishing. https://doi.org/10.1109/ICPE.2015.7167792

Marouchos, C. C. (2006). The buck boost DC to DC converter. In *The Switching Function: Analysis of Power Electronic Circuits* (pp. 163–174). The Institution of Engineering and Technology. https://doi.org/10.1049/PBCS017E_CH11

Muntaser, A., Ragb, H., & Elwrfalli, I. (2022). *DC Microgrid Based on Battery, Photovoltaic, and Fuel Cells; Design and Control*. arXiv Preprint. https://doi.org/10.20944/preprints202212.0527.v1

Raghavendra, N. K., & Padmavathi, K. (2018). Solar charge controller for lithium-ion battery. In *2018 IEEE International Conference on Power Electronics, Drives and Energy Systems (PEDES)* (pp. 1-5). IEEE Publishing. https://doi.org/10.1109/PEDES.2018.8707743

Rokonuzzaman, M., Shakeri, M., Hamid, F. A., Mishu, M. K., Pasupuleti, J., Rahman, K. S., Tiong, S. K., & Amin, N. (2020). IoT-enabled high efficiency smart solar charge controller with maximum power point tracking - Design, hardware implementation and performance testing. *Electronics*, *9*(8), 1–16. https://doi.org/10.3390/electronics9081267

Wang, L. Y., Zhao, M. L., & Wu, X. B. (2016). A monolithic high-performance buck converter with enhanced current-mode control and advanced protection circuits. *IEEE Transactions on Power Electronics*, *31*(1), 793–805. https://doi.org/10.1109/TPEL.2015.2405093

Wang, N., Hu, R., & Zhu, M. (2019). *Methods to Solve Reverse Current Caused Damage in Synchronous Buck Converter* (Application Report). Texas Instruments. https://www.ti.com/lit/an/slua962/slua962.pdf?ts=1736996669125&ref_url=https%253A%252F%252Fwww.google.com%252F

Xu, F., Liu, J., & Dong, Z. (2022). Minimum backflow power and ZVS design for dual-active-bridge DC-DC converters. *IEEE Transactions on Industrial Electronics, 70*(1), 474-484. https://doi.org/10.1109/TIE.2022.3156159

Zomorodi, H., & Nazari, E. (2022). Design and simulation of synchronous buck converter in comparison with regular buck converter. *International Journal of Robotics and Control Systems*, *2*(1), 79–86. https://doi.org/10.31763/ijrcs.v2i1.538